

RESEARCH ARTICLE

Enhancing regeneration after acute kidney injury by promoting cellular dedifferentiation in zebrafish

Lauren Brill Skvarca^{1,2,*}, Hwa In Han^{1,*}, Eugenel B. Espiritu¹, Maria A. Missinato^{1,3}, Elizabeth R. Rochon⁴, Michael D. McDaniels¹, Abha S. Bais¹, Beth L. Roman⁵, Joshua S. Waxman⁶, Simon C. Watkins⁷, Alan J. Davidson⁸, Michael Tsang¹ and Neil A. Hukriede^{1,9,‡}

ABSTRACT

Acute kidney injury (AKI) is a serious disorder for which there are limited treatment options. Following injury, native nephrons display limited regenerative capabilities, relying on the dedifferentiation and proliferation of renal tubular epithelial cells (RTECs) that survive the insult. Previously, we identified 4-(phenylthio)butanoic acid (PTBA), a histone deacetylase inhibitor (HDI), as an enhancer of renal recovery, and showed that PTBA treatment increased RTEC proliferation and reduced renal fibrosis. Here, we investigated the regenerative mechanisms of PTBA in zebrafish models of larval renal injury and adult cardiac injury. With respect to renal injury, we showed that delivery of PTBA using an esterified prodrug (UPHD25) increases the reactivation of the renal progenitor gene *Pax2a*, enhances dedifferentiation of RTECs, reduces Kidney injury molecule-1 (Kim-1) expression, and lowers the number of infiltrating macrophages. Further, we found that the effects of PTBA on RTEC proliferation depend upon retinoic acid signaling and demonstrate that the therapeutic properties of PTBA are not restricted to the kidney but also increase cardiomyocyte proliferation and decrease fibrosis following cardiac injury in adult zebrafish. These studies provide key mechanistic insights into how PTBA enhances tissue repair in models of acute injury and lay the groundwork for translating this novel HDI into the clinic.

This article has an associated First Person interview with the joint first authors of the paper.

KEY WORDS: Acute kidney injury, Macrophages, Renal proximal tubule cell, Cardiovascular, HDAC inhibitor, Therapeutic

¹Department of Developmental Biology, University of Pittsburgh, Pittsburgh, PA 15261, USA. ²Department of Pathology, University of Pittsburgh, Pittsburgh, PA 15213, USA. ³Sanford Burnham Prebys Medical Discovery Institute, La Jolla, CA 92037, USA. ⁴Pittsburgh Heart, Lung, and Blood Vascular Medicine Institute, Department of Medicine, University of Pittsburgh, Pittsburgh, PA 15261, USA. ⁵Human Genetics, Graduate School of Public Health, University of Pittsburgh, Pittsburgh, PA 15261, USA. ⁶Heart Institute, Molecular Cardiovascular Biology Division, Cincinnati Children's Hospital Medical Center, Cincinnati, OH 45229, USA. ⁷Department of Cell Biology and Center for Biological Imaging, University of Pittsburgh, Pittsburgh, PA 15261, USA. ⁸Molecular Medicine and Pathology, University of Auckland, Auckland, New Zealand. ⁹Center for Critical Care Nephrology, University of Pittsburgh, Pittsburgh, PA 15213, USA.

*These authors contributed equally to this work

‡Author for correspondence (hukriede@pitt.edu)

© A.S.B., 0000-0001-5910-1306; J.S.W., 0000-0002-8132-487X; N.A.H., 0000-0002-9655-9030

This is an Open Access article distributed under the terms of the Creative Commons Attribution License (<https://creativecommons.org/licenses/by/4.0/>), which permits unrestricted use, distribution and reproduction in any medium provided that the original work is properly attributed.

Received 3 October 2018; Accepted 11 March 2019

INTRODUCTION

Acute kidney injury (AKI) is a rapid decline in renal function that results in 2 million deaths annually worldwide and accounts for billions of dollars in US healthcare costs (Chertow et al., 2005; Murugan and Kellum, 2011). AKI frequently occurs in a hospitalized setting, where 3–20% of patients are affected (Fang et al., 2010; Uchino et al., 2006). It is even more common in the intensive care unit, with up to 67% of patients affected (Bagshaw et al., 2008; Cruz et al., 2007; Hoste et al., 2006; Ostermann and Chang, 2007). It is now recognized that AKI may not be an isolated event; rather, many patients who recover clinically do not regain baseline renal function and are at increased risk for developing chronic kidney disease (Chawla and Kimmel, 2012; Coca et al., 2012; Kjellstrand et al., 1981; Liaño et al., 2007; Venkatachalam et al., 2010).

AKI represents a disease spectrum with numerous contributing causes (Levey and James, 2017). Since renal biopsies are not often performed in AKI patients, the underlying physiology and histopathology have been largely defined using rodent models (Lieberthal and Nigam, 2000; Murugan and Kellum, 2011). These studies have identified key cellular players during AKI events, including roles for the tubular epithelium and the immune system. Specifically, damaged renal tubular epithelial cells (RTECs) undergo dedifferentiation to a mesenchymal state by reactivating pathways common during early renal development (Benigni et al., 2010; Cirio et al., 2014; Imgrund et al., 1999; Lin et al., 2010; Terada et al., 2003; Villanueva et al., 2006; Witzgall et al., 1994). These surviving RTECs proliferate and repopulate areas of lost cells in the nephron (Humphreys et al., 2008). Additionally, injured RTECs activate an immune response by increased expression of Toll-like receptors and production of pro-inflammatory cytokines to attract leukocytes to the kidney (Wolfs et al., 2002; Wu et al., 2007). These signals result in the rapid activation of the innate immune system, with neutrophils arriving within 30 min of ischemia-reperfusion (IR-AKI) injury (Awad et al., 2009; Kelly et al., 1996; Li et al., 2008; Rabb et al., 1994; Thornton et al., 1989). In addition, heterogeneous macrophage populations participate in both tissue injury and repair (Cao et al., 2015; Ricardo et al., 2008). Early in the course of renal injury, pro-inflammatory macrophages (called either classically activated or M1) infiltrate the kidney and perpetuate damage by secreting pro-inflammatory cytokines and producing reactive oxygen species (ROS) (Cao et al., 2015; Jo et al., 2006; Lee et al., 2011). Subsequently, phagocytosis of cellular debris and other environmental cues trigger suppression of M1 macrophages and promote polarization toward a reparative macrophage phenotype (called either alternatively activated or M2) (Cao et al., 2015; Lee et al., 2011). M2 macrophages are generally considered to promote tissue repair, proliferate *in situ* (Zhang et al., 2012), protect RTECs from apoptosis and promote cell cycle progression (Lin et al., 2010; Schmidt et al., 2013; Sola et al.,

2011). These coordinated responses are critical for nephron repair and recovery from AKI (Han et al., 2019).

Despite advancements in understanding AKI pathophysiology, there is an unmet need for clinical therapies. No targeted clinical treatments are currently available that accelerate renal recovery or decrease fibrosis when administered after injury. We previously identified 4-(phenylthio)butanoic acid (PTBA), a novel short-chain carboxylic acid class histone deacetylase inhibitor (HDI), which are considered HDAC class-I specific (de Groh et al., 2010; Fass et al., 2011). We previously evaluated the therapeutic potential of PTBA, delivered as a prodrug of either a methyl ester (UPHD25) or amide (UPHD186) (Cianciolo Cosentino et al., 2013; Skrypnik et al., 2016). In zebrafish and mouse models of AKI, we have shown that PTBA enhances survival, increases RTEC proliferation, ameliorates injury and reduces renal scarring (Cianciolo Cosentino et al., 2013; Novitskaya et al., 2014; Skrypnik et al., 2016). Importantly, PTBA was efficacious when delivered post-AKI in all animal models, heightening the potential for clinical applicability.

In this study, we utilized the optical transparency of zebrafish larvae to characterize the cellular mechanisms by which PTBA enhances the regenerative response following AKI. Since we have previously shown that PTBA exhibits similar efficacy in both zebrafish and mammalian AKI models, here we focus on zebrafish AKI studies, as we can easily and precisely deliver the compound to zebrafish larvae and subsequently track cell populations by both static- and live-imaging methods. We demonstrate that delivering PTBA as a prodrug (UPHD25) increases RTEC dedifferentiation, attenuates tubular injury, lowers total macrophage recruitment and decreases the number of inflammatory (M1) macrophages. We found that the pro-regenerative effects of PTBA depend on intact retinoic acid (RA) signaling, in line with HDACs being modulators of RA signaling and this pathway playing a key early role in kidney regeneration (Brilli et al., 2013; Chiba et al., 2016). Finally, we looked at the applicability of PTBA to enhance cardiac repair, another RA-dependent model of regeneration (Kikuchi et al., 2011), and found that treatment promotes cardiomyocyte proliferation and decreases fibrosis. Overall, these studies provide insight into the cellular mechanism underlying PTBA-driven regeneration.

RESULTS

PTBA increases RTEC dedifferentiation and proliferation post-AKI

We have previously shown that PTBA treatment increases the number of RTECs in active cell cycle in a zebrafish larval model of AKI (Cianciolo Cosentino et al., 2013; Hentschel et al., 2005). To assess whether PTBA increases the population of cells that show AKI-mediated reactivation, we examined whether post-AKI UPHD25 treatment increases expression of Pax2a, a critical early developmental transcription factor for RTEC dedifferentiation (Humphreys et al., 2011; Imgrund et al., 1999; Maeshima et al., 2002; Villanueva et al., 2006). Larvae were injected with gentamicin (gent-AKI) between 78 and 82 hours post-fertilization (hpf), followed by a single-dose UPHD25 treatment at 2 days post injection (dpi) (Fig. 1A). To identify proximal tubules (PTs), we used the *Tg(PT:EGFP)* line (Cianciolo Cosentino et al., 2013). There is little Pax2a expression in uninjured larvae RTECs, and UPHD25 treatment of uninjured larvae does not cause Pax2a reactivation (Fig. 1B,C,F). In gent-AKI larvae, Pax2a is reactivated in RTECs within 48 h after gentamicin injection and expression is maintained in a population of RTECs through at least 3 dpi (Fig. 1D-F). When gent-AKI larvae are treated with UPHD25, the number of Pax2a-positive RTECs significantly increases, as assayed both by immunofluorescence and transcript levels (Fig. 1D-F,

Fig. S1A). To demonstrate that Pax2a is expressed in proliferating cells in zebrafish larvae in AKI, as has been shown in murine models (Humphreys et al., 2011), we co-stained for Pax2a and proliferating cell nuclear antigen (PCNA), which marks cells in S-phase. Both UPHD25 and dimethyl sulfoxide (DMSO)-treated injured larvae show double-positive cells, but UPHD25-treated fish exhibit a higher number of double-positive cells than DMSO-treated fish. (Fig. 1G-I). These results suggest that UPHD25 increases selective Pax2a reactivation and concomitant cellular proliferation in an injury setting.

UPHD25 treatment increases dedifferentiation and ameliorates injury

To confirm that Pax2a reactivation is associated with dedifferentiation of RTECs, we examined the effect of PTBA on Vimentin expression, an intermediate-filament protein that increases in dedifferentiated RTECs after AKI (Witzgall et al., 1994). We treated gent-AKI *Tg(PT:EGFP)* fish with DMSO or UPHD25 at 2 dpi and examined co-expression of Vimentin and Pax2a. Uninjured, control larvae did not show Vimentin staining, while gent-AKI resulted in Vimentin expression in Pax2a+ cells (Fig. 2A,B). Gent-AKI+UPHD25 showed significantly increased Vimentin expression when compared to gent-AKI+DMSO-treated fish via both immunofluorescence and transcript levels (Fig. 2B-D, Fig. S1B). As further evidence that dedifferentiation is enhanced with UPHD25 treatment, we performed RNA-seq transcriptome profiling of epithelial-to-mesenchymal transition (EMT) markers (Grande et al., 2015; Lovisa et al., 2015) (see supplemental methods). In isolated PTs from injured kidneys treated with either DMSO or UPHD25, there was a trend of downregulation of known epithelial markers and a trend of upregulation of mesenchymal markers in those larvae treated with UPHD25 as compared to the DMSO controls (Fig. S1D). Together with an increased expression of Pax2 and Vimentin, these changes in expression of EMT markers further validate the observation that UPHD25 treatment enhances dedifferentiation in RTECs.

Since treatment increases dedifferentiation and proliferation of PT cells, we examined the effect of PTBA on levels of Kidney injury molecule-1 (Kim-1) expression, which increases in RTECs after AKI and also plays a role in fibrosis and leukocyte recruitment (Humphreys et al., 2013; Ichimura et al., 1998). Following gent-AKI in zebrafish larvae, robust Kim-1 staining is detectable in injured fish by 2 dpi (Chiba et al., 2016). To quantify Kim-1 protein, we measured the percent area of fluorescence within the tubule as well as *kim-1* mRNA expression levels (Fig. 3A-C, Fig. S1C). Compared to gent-AKI+DMSO, the gent-AKI+UPHD25 group showed a decrease in renal Kim-1 protein expression and transcript levels at 3 dpi (Fig. 3B-D, Fig. S1C). Collectively, the data demonstrate that Pax2a reactivation occurs in dedifferentiated RTECs after gentamicin injury, and that PTBA mitigates cellular injury in RTECs.

Immune system response in zebrafish gent-AKI

Activation of Kim-1 in RTECs has been associated with a prolonged inflammatory response and fibrosis in mice (Humphreys et al., 2013). Thus, we determined whether PTBA affects the leukocyte response in the zebrafish gent-AKI model. In mammals, AKI results in the rapid influx of neutrophils and macrophages (Cao et al., 2015; Jo et al., 2006; Lee et al., 2011; Li et al., 2008; Ricardo et al., 2008), but these responses have not yet been characterized during AKI in zebrafish. Since the innate immune response is functional in zebrafish larvae by 3 dpf (Keightley et al., 2014), we first determined whether neutrophils and macrophages also infiltrate the pronephric kidney after gent-AKI. To evaluate the neutrophil response, we performed time-lapse

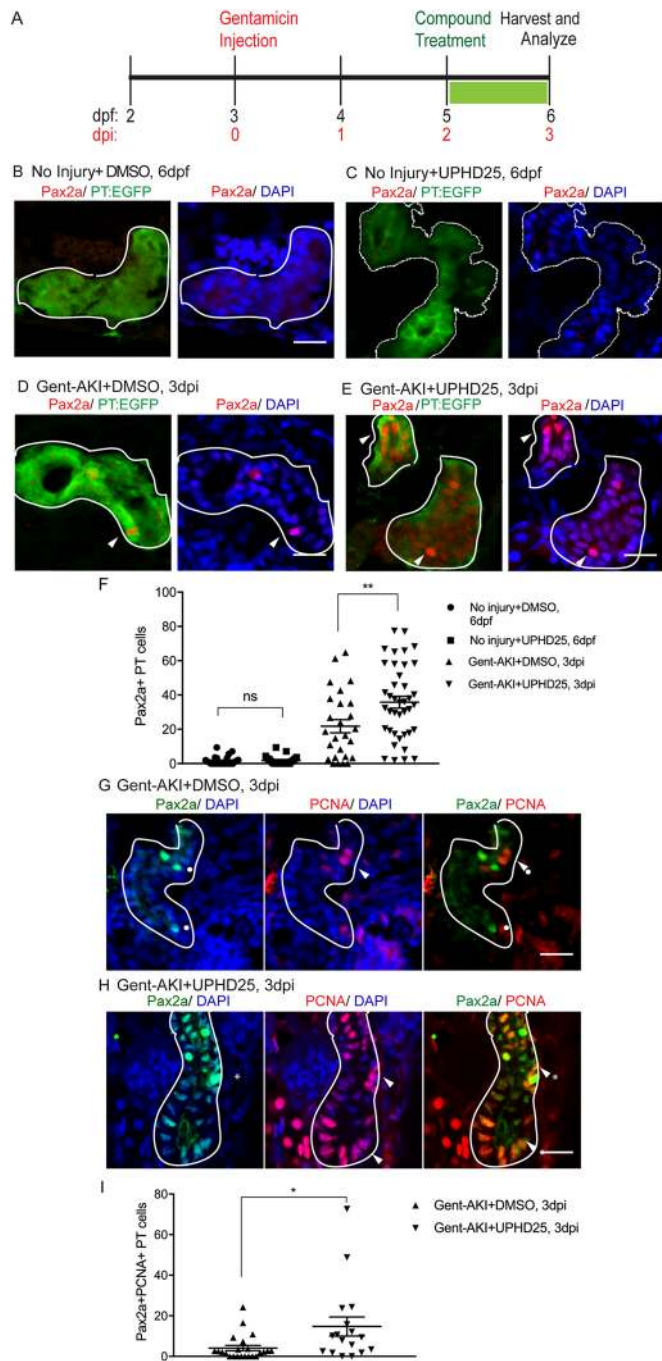


Fig. 1. UPHD25 treatment increases Pax2a reactivation and proliferation during AKI. (A) Experiment schematic: *Tg(PT:EGFP)* larvae were injected with gentamicin at 3 dpf to induce AKI (gent-AKI). At 2 dpi, gent-AKI larvae were treated with 1% DMSO or 1 μ M UPHD25 for 24 h (2-3 dpi) then harvested for analysis. (B-E) Immunofluorescence staining of Pax2a (red), proximal tubule (PT; green) and nuclei (DAPI; blue) of age-matched 6 dpf no injury+DMSO (B), 6 dpf no injury+UPHD25 (C), 3 dpi gent-AKI+DMSO (D) and 3 dpi gent-AKI+UPHD25 (E) larvae. Nuclear localization of Pax2a was shown by overlaying with nuclear counterstain, DAPI (blue). PT is outlined in white and Pax2a+ RTECs are marked with arrowheads. (F) Quantification of Pax2a+ cells. Mean_{NoInjury+DMSO}=1.561 (N=26) vs Mean_{NoInjury+UPHD25}=1.787 (N=21) vs Mean_{Gent-AKI+DMSO}=21.8 (N=26) vs Mean_{Gent-AKI+UPHD25}=35.79 (N=40). Data pooled from three biological replicates are shown expressed as mean \pm s.e.m. One-way ANOVA. (G,H) Immunofluorescence co-stain of Pax2a (green), PCNA (red) and DAPI (blue) in gent-AKI+DMSO (G) and gent-AKI+UPHD25 (H). Nuclear localization of PCNA was shown by overlaying with nuclear counterstain, DAPI (blue). Pax2a+ cells are marked with asterisks and PCNA+ are marked with arrowheads. (I) Quantification of Pax2a+ PCNA+ cells. Mean_{Gent-AKI+UPHD25}=4.08 (N=23) vs Mean_{Gent-AKI+UPHD25}=14.74 (N=17). Data pooled from three biological replicates are shown expressed as mean \pm s.e.m. Two-tailed t-test: * P <0.05, ** P <0.01, ns, not significant. Scale bars: 20 μ m.

(Fig. 4D). However, gent-AKI larvae showed significantly more renal neutrophils at both 5 dpf (2 dpi) and 6 dpf (3 dpi), compared to uninjured controls (Fig. 4D).

We performed similar imaging and histology studies to evaluate the macrophage response. To visually detect macrophages, we utilized the transgenic reporter line *Tg(mpeg1:dendra2)*, in which macrophages are green (Harvie et al., 2013). We performed live time-lapse imaging in *Tg(cdh17:mCherry); Tg(mpeg1:dendra2)* double-transgenic fish after gentamicin injection (Fig. 4E). We captured z-stack images of the PT region over 20 h beginning at 48 hpi and observed an influx of macrophages to the PT in gent-AKI fish. Uninjured fish display Dendra2+ macrophages circulating rapidly; however, only a few macrophages make prolonged contact with the PT (Fig. 4F, Movie 3). In contrast, gent-AKI fish show recruitment and retention of many macrophages to the mCherry+ kidney epithelium (Fig. 4F, Movie 4). To quantify this response, we fixed *Tg(mpeg1:dendra2); Tg(PT:EGFP)* double-transgenic fish and counted the number of Dendra2+ macrophages adjacent to the PT (Fig. 4G). Compared to uninjured fish, gent-AKI larvae showed an increased number of renal macrophages at 3 dpi (Fig. 4G,H). Taken together, these data indicate that the gent-AKI zebrafish larvae show a robust innate immune response between 2 and 3 dpi.

Effect of PTBA on the immune system

Having characterized the timing of neutrophil and macrophage influx during gent-AKI in zebrafish larvae, we assessed whether PTBA affects the innate immune response. We treated gent-AKI *Tg(lyz:EGFP)* or *Tg(mpeg1:dendra2)* fish with DMSO or UPHD25, and quantified renal neutrophils and macrophages at 3 dpi (Fig. 5A,B). At this time point, there was no significant change in the number of neutrophils, but there was a small but significant decrease in the number of macrophages between treatment groups. This suggests that UPHD25 treatment does not affect initial neutrophil recruitment but may decrease the overall number of macrophages that are recruited to the PT (Fig. 5C,D).

Since the *mpeg1* transgenic line marks multiple macrophage phenotypes, we wanted to determine whether UPHD25 treatment affected macrophage polarization (Cao et al., 2015; Jo et al., 2006; Lee et al., 2011). Studies have shown that zebrafish undergo M1/M2 polarization akin to their mammalian counterparts (Nguyen-Chi et al., 2015; Wiegertjes et al., 2016). Therefore, we utilized the *Tg(mpeg1:dendra2)* line and stained for TNF α , an M1-specific

confocal imaging in gent-AKI transgenic fish expressing mCherry driven by the *cadherin-17* promoter, *Tg(cdh17:mCherry)*, a renal tubule marker (Sanker et al., 2013), and enhanced GFP driven by the *lysozyme C* promoter, *Tg(lyz:EGFP)*, a marker of neutrophils (Fig. 4A) (Ellett et al., 2011; Kitaguchi et al., 2009). We captured z-stack images of the PT region over 17 h beginning at 24 hours post-injury (hpi). In uninjured fish, EGFP+ neutrophils move rapidly, with few cells accumulating near the PT (Fig. 4B, Movie 1). In contrast, neutrophils in gent-AKI fish move slowly, and several migrated adjacent to the mCherry-positive kidney epithelium (Fig. 4B, Movie 2). In order to quantify the response, we acquired samples at several time points and quantified EGFP+ neutrophils adjacent to the PT by examining serial sections (Fig. 4C). At 4 dpf (1 dpi), there is no change in the number of renal neutrophils after gentamicin injection

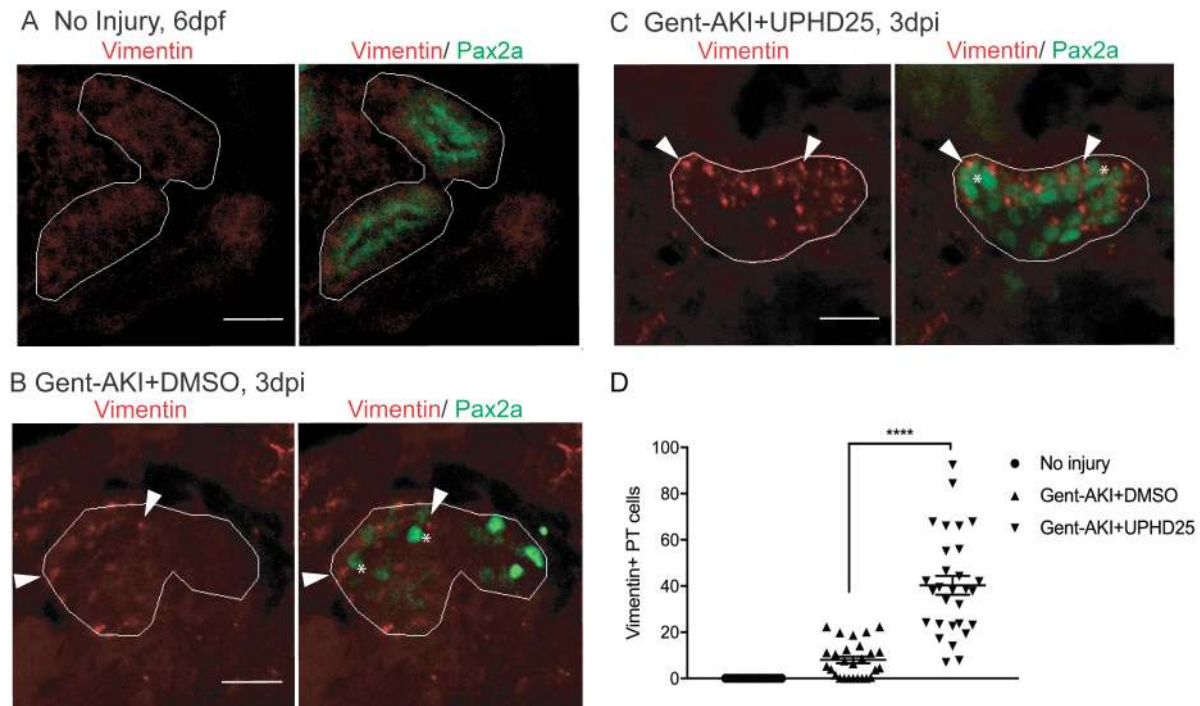


Fig. 2. UPHD25 treatment increases dedifferentiation during AKI. (A-C) Immunofluorescence co-stain of Vimentin (red; cytosolic) and Pax2a (green) in PT of age-matched 6-dpf no injury (A), 3 dpi gent-AKI+DMSO (B) and 3 dpi gent-AKI+UPHD25 (C) fish. (D) Quantification of Vimentin+ RTECs. Mean_{NoInjury+UPHD25}=0 (N=22) vs Mean_{Gent-AKI+DMSO}=8.00 (N=27) vs Mean_{Gent-AKI+UPHD25}=40.31 (N=29). Pax2a+ cells are marked with asterisks and Vimentin+ RTECs are marked with arrowheads. PT is outlined in white. Data pooled from three biological replicates are shown expressed as mean \pm s.e.m. One-way ANOVA: **** P <0.001. Scale bars: 20 μ m.

pro-inflammatory cytokine (Fig. 6A-C) (Nelson et al., 2013). Since other pro-inflammatory cells also express TNF α , we quantified the ratio of cells that co-labelled TNF α +mpeg1:Dendra2+. In gent-AKI+DMSO-treated fish, many M1 macrophages are recruited to RTECs, while gent-AKI+UPHD25-treated fish display fewer M1 macrophages (Fig. 6A-C). To quantify M2 macrophages, we utilized the same method, but used an M2-specific enzyme, Arginase-2 (Fig. S2; see supplemental methods) (Wiegertjes et al., 2016). Comparing gent-AKI+DMSO- with gent-AKI+UPHD25-treated fish, we found no significant change in the number of M2 macrophages in the renal field (Fig. 6D-F). Overall, these results suggest that PTBA reduces total macrophage recruitment and the number of inflammatory macrophages recruited to the damaged tubule.

Effect of PTBA on proximal tubular cell proliferation requires intact RA signaling

Among various pathways critical for macrophage response, the RA pathway has been implicated in macrophage recruitment during AKI (Chiba et al., 2016). Moreover, HDI treatments in mammalian AKI suppress inflammation and fibrosis, thereby improving long-term outcomes (Kinugasa et al., 2010; Marumo et al., 2010). Therefore, we determined whether PTBA required RA activity for efficacy in the zebrafish gent-AKI model. We treated gent-AKI *Tg(PT:EGFP)* fish with Ro41-5253 (abbreviated Ro41), an RA receptor (RAR) antagonist that effectively blocks RA signaling in zebrafish larvae (Chiba et al., 2016). We analyzed proliferation by performing immunofluorescence and quantifying the number of PCNA+ RTECs. In DMSO-treated larvae, Ro41-5253 did not significantly alter the number of PCNA+ RTECs compared to untreated larvae (Fig. 7A,B,E). UPHD25 treatment increased the number of PCNA+ RTECs, while co-treatment with Ro41-5253

and UPHD25 significantly decreased PCNA+ RTECs compared to UPHD25 treatment alone (Fig. 7C-E). Therefore, Ro41-5253 effectively blocks PTBA efficacy, suggesting that treatment requires intact RAR signaling to stimulate RTEC proliferation.

To confirm the specificity of Ro41-5253, we utilized an inducible transgenic zebrafish line, *Tg(hsp70l:EGFP-HS-dnRAR α)*, in which heat shock stimulates expression of a dominant-negative form of the human RAR- α (DN-RAR α ; see supplemental methods) (Pogoda et al., 2018; Waxman et al., 2008; Waxman and Yelon, 2011). We previously showed that UPHD25 treatment increased active RTEC proliferation in uninjured larvae (Cianciolo Cosentino et al., 2013). Therefore, we evaluated whether reducing RA signaling in this heat-inducible transgenic model would block UPHD25-stimulated RTEC proliferation. Uninjured *Tg(hsp70l:EGFP-HS-dnRAR α)* larvae were heat shocked for 1 h at 5 dpf then treated with either DMSO or UPHD25 for 24 h. We quantified PCNA at 6 dpf and compared proliferation to wild-type larvae treated with DMSO or UPHD25 (Fig. S3A-E). Proliferation rates were comparable between heat-shocked (+HS) and non-heat-shocked (-HS) larvae treated with DMSO (Fig. S3A,B); however, UPHD25 -HS treatment showed impaired RTEC proliferation compared to UPHD25 +HS (Fig. S3C,D). Therefore, in uninjured larvae, UPHD25 requires RA signaling to stimulate RTEC proliferation. Similarly, we evaluated proliferation in this transgenic model after AKI at 3 dpf. At 2 dpi, larvae were heat shocked for 1 h and then treated with DMSO or UPHD25 for 24 h (Fig. S3F-J). Overall, gent-AKI larvae showed higher proliferation than the no-injury group, suggesting that injury results in increased proliferation. Within the gent-AKI group, proliferation rates were comparable between DMSO +HS and DMSO -HS (Fig. S3F,G). However, gent-AKI +UPHD25 +HS showed impaired RTEC proliferation compared to UPHD25 -HS controls (Fig. S3H,I).

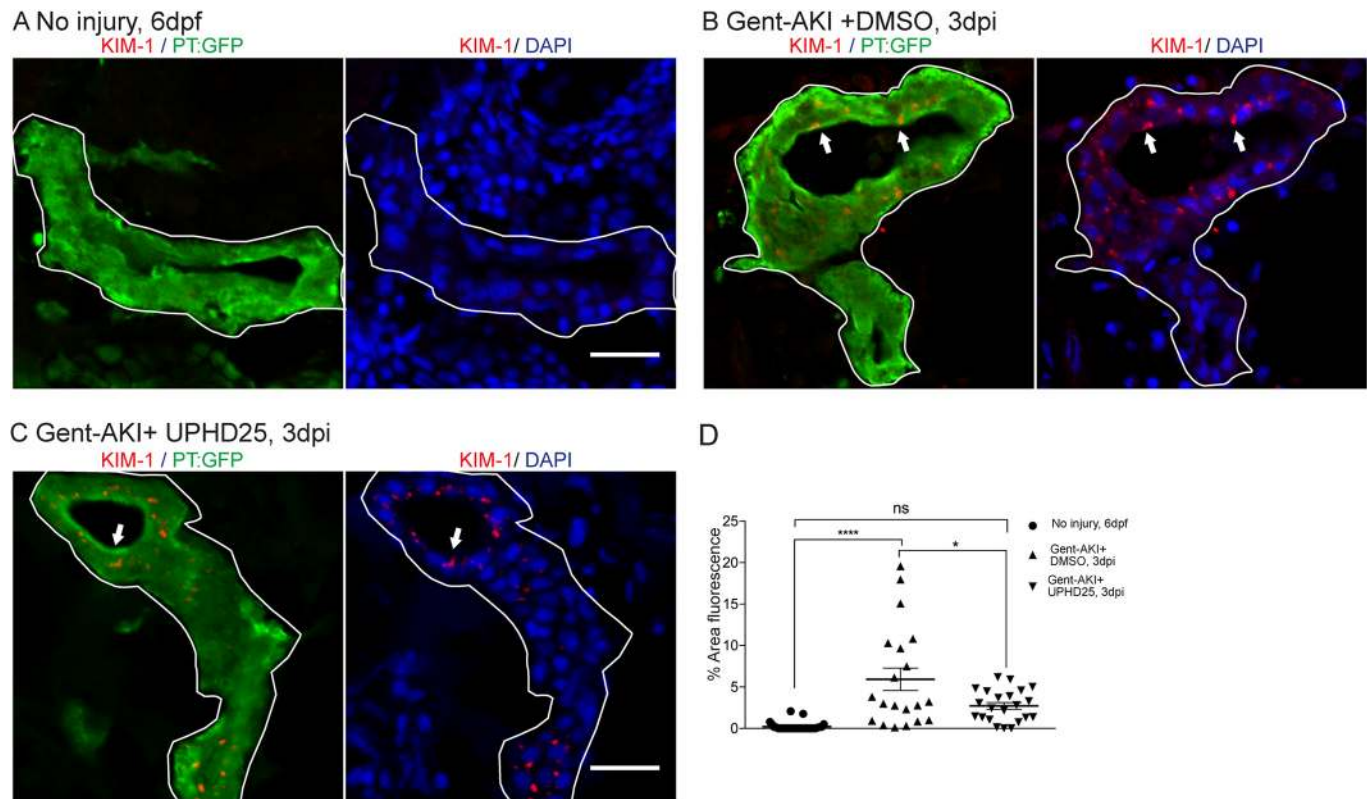


Fig. 3. UPHD25 treatment decreases Kim-1 expression level after AKI. (A) Immunofluorescence of Kim-1 expression in 6 dpf uninjured (A), 3 dpi gent-AKI +DMSO (B) and 3 dpi gent-AKI +UPHD25 (C) larvae. Apical localization of Kim-1 was shown by overlaying with nuclear counterstain, DAPI (blue). Histological sectioning poses a challenge of obtaining a perpendicular transversal cut to observe Kim-1 apical localization. (C) Shows an ideal perpendicular transversal section to observe apical expression of Kim-1. PTs are outlined in white and RTECs with Kim-1 expression are marked with arrows. (D) Quantification of Kim-1 was acquired via measuring the area of Kim-1 expression in PTs. Mean_{NoInjury}=0.22 (N=29) vs Mean_{Gent-AKI+DMSO}=5.92 (N=20) vs Mean_{Gent-AKI+UPHD25}=2.71 (N=22). Data pooled from three biological replicates are shown expressed as mean±s.e.m. One-way ANOVA: *P<0.05, ****P<0.001, ns, not significant. Scale bars: 20 μm.

Therefore, either pharmacologic or genetic inhibition of RAR signaling significantly reduces UPHD25 efficacy. Taken together, these data indicate that the mechanism of action of PTBA requires upstream RA signaling.

Additionally, we evaluated treatment in an adult zebrafish model of cardiac injury (Poss et al., 2002), in which RA signaling has been shown to be essential for regeneration (Kikuchi et al., 2011). Adult zebrafish recover from this procedure within 30-60 days and recovery relies on the regenerative capacity of proliferating cardiomyocytes, which peaks around 7 days post-amputation (dpa) (Jopling et al., 2010; Kikuchi et al., 2010; Poss et al., 2002). At 1 dpa, adult zebrafish were treated daily with 200 μM UPHD25 until 6 dpa (see supplemental methods) (Missinato et al., 2015; Pugach et al., 2009). We evaluated cardiomyocyte proliferation at 7 dpa by staining for Mef2c, a marker of cardiomyocytes, and PCNA (see supplemental methods; Fig. S4A-C). UPHD25 treatment did not affect cardiomyocyte proliferation in uninjured fish (Fig. S4A,C), suggesting that PTBA does not affect non-injured, differentiated cells in adult tissue. After cardiac injury, UPHD25 treatment significantly increases the number of proliferating cardiomyocytes (Fig. S4B,C). To determine whether increased cardiomyocyte proliferation is associated with long-term beneficial effects, we performed acid fuchsin Orange G (AFOG) staining after cardiac injury and quantified the fibrotic clot size at 20 dpa (see supplemental methods; Fig. S4D). Compared to DMSO-treated controls, UPHD25-treated fish showed a significant reduction in clot size, indicating acceleration of recovery (Fig. S4D,E). Taken together, these data

show that PTBA improves recovery after cardiac injury by increasing cardiomyocyte proliferation and decreasing fibrosis.

DISCUSSION

In this study, we showed that treatment with the PTBA prodrug UPHD25 enhances recovery after gent-AKI in zebrafish larvae by ameliorating tubular injury and stimulating RTEC dedifferentiation and proliferation. This work demonstrates that PTBA is a useful chemical probe to dissect early post-repair processes in RTECs involving dedifferentiation and proliferation. PTBA treatment also increased cardiomyocyte proliferation following heart injury. Taken together, these studies indicate that PTBA may possess broad therapeutic potential across multiple organ injury models.

There is evidence that cellular stress following injury results in cell-cycle arrest of RTECs (Yang et al., 2010). Prolonged cell-cycle arrest at either G1/S or G2/M checkpoints promotes maladaptive tubular responses associated with impaired repair and increased fibrosis after AKI (Ferenbach and Bonventre, 2015; Kellum and Chawla, 2016). We previously determined that PTBA drives an increase in the number of actively proliferating tubular epithelial cells and reduces the number of tubular epithelial cells in G2/M (Cianciolo Cosentino et al., 2013; Novitskaya et al., 2014). Since post-AKI fibrosis is thought to result from the accumulation of injured tubular epithelial cells in G2/M (Lin et al., 2010; Liu et al., 2013; Varmeh et al., 2011; Yang et al., 2010; Zahedi et al., 2006), these data suggest that PTBA reduces fibrosis by promoting effective tubular repair by more cells progressing through the G2/M

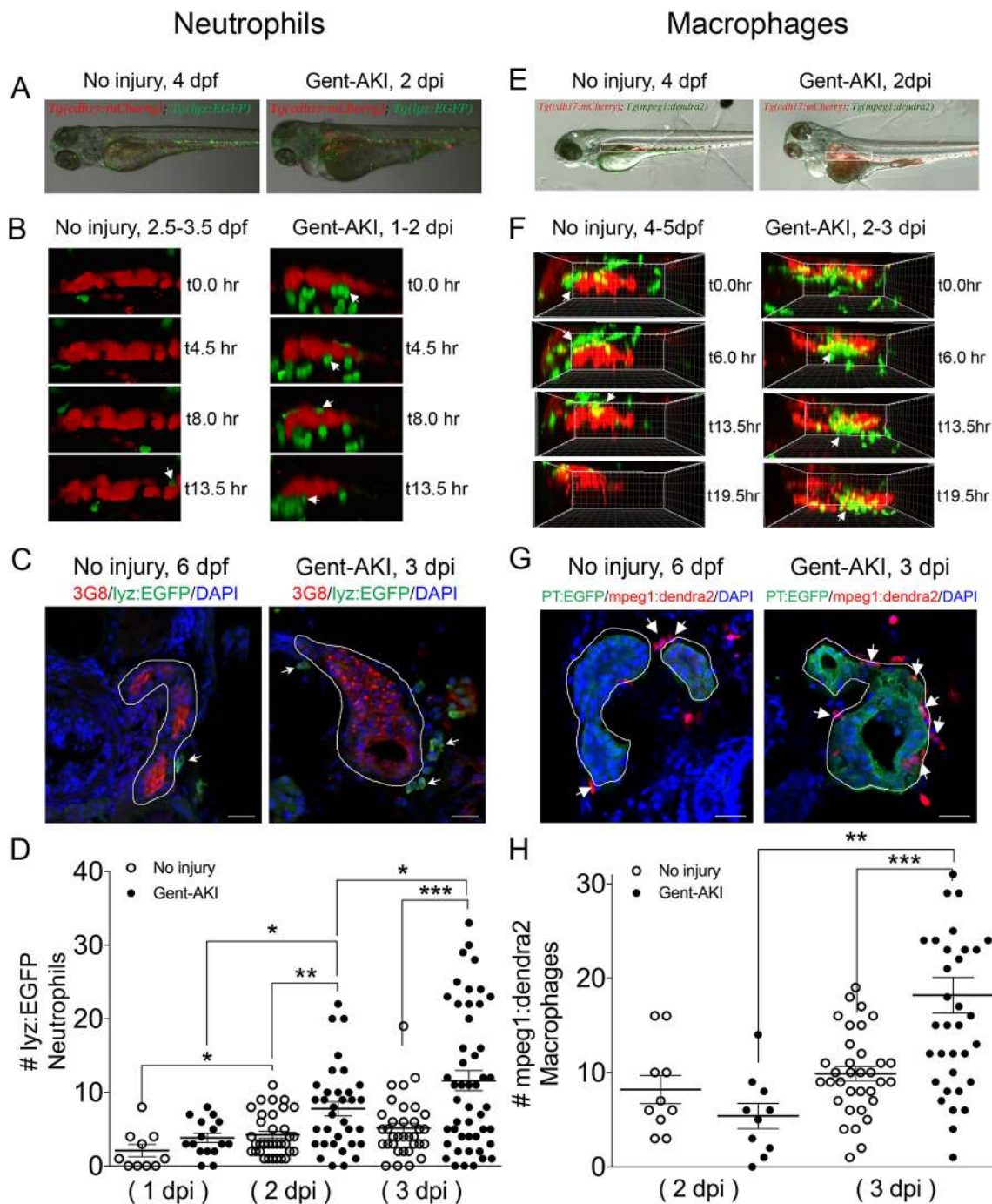


Fig. 4. Neutrophil and macrophage populations change in the kidney field after AKI. (A-D) *Tg(cdh17:mCherry); Tg(lyz:EGFP)* transgenic zebrafish were used for neutrophil analyses. (E-H) *Tg(cdh17:mCherry); Tg(mpeg1;dendra2)* transgenic zebrafish were used for macrophage analyses. (A,E) Transgenic lines were injected with gentamicin at 3 dpf and imaged at 2 dpi. (B,F) Snapshots of live imaging of *lyz*⁺ neutrophils imaged at 1 dpi for 13.5 h (B) and *mpeg1*⁺ macrophages imaged at 2 dpi for 19.5 h (F) in a no-injury and gent-AKI setting. Arrows indicate neutrophils or macrophages adjacent to PTs. (C,G) Immunofluorescence co-stain of PTs (red or green) and neutrophils (green) (C) or macrophages (red) (G) in no-injury and gent-AKI at 3 dpi. PTs are outlined in white and adjacent leukocytes are marked with arrows. (D,H) Quantification of neutrophil (D) and macrophage (H) numbers adjacent to the PT before and after injury. Mean_{NoInjury5dpf}=4.24 (N=34) vs Mean_{2dpi}=7.76 (N=34) vs Mean_{NoInjury6dpf}=5.15 (N=34) vs Mean_{3dpi}=11.60 (N=48). Adjacent leukocytes were counted for both no injury and gent-AKI at 1, 2 and 3 dpi (D), and 2 and 3 dpi (H). Data pooled from three biological replicates are shown expressed as mean±s.e.m. One-way ANOVA: **P*<0.05, ***P*<0.01, ****P*<0.005. Scale bars: 20 μm.

checkpoint and increasing proliferation. In various acute injury settings, cells that undergo proliferation are thought to originate from dedifferentiating cells (Bonventre, 2003; He et al., 2013; Wang et al., 2017). Our findings demonstrate that PTBA induces an increase in Pax2a and Vimentin expression, known markers of

RTEC dedifferentiation, as well as an increase in mesenchymal genes and a reduction in epithelial genes (Grande et al., 2015; Imgrund et al., 1999; Lovisa et al., 2015; Maeshima et al., 2002; Witzgall et al., 1994). Overall, this panel of markers provides a clear demonstration that the effects of PTBA occur through an EMT

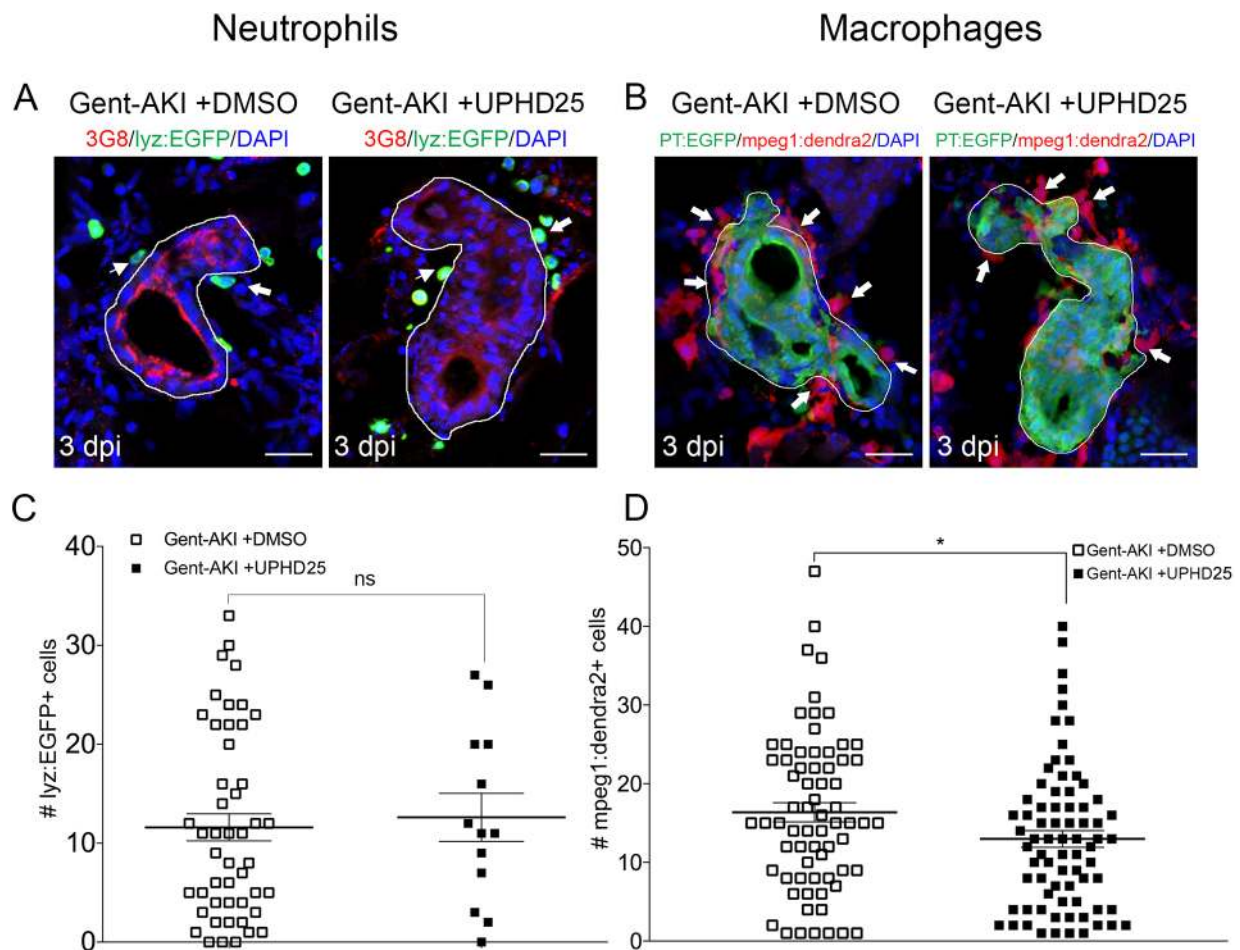


Fig. 5. UPHD25 treatment has no effect on neutrophil response but lowers total macrophage recruitment during early AKI phase. (A,C) *Tg(cdh17:mCherry); Tg(lyz:EGFP)* transgenic zebrafish were used for neutrophil analyses. (B,D) *Tg(cdh17:mCherry); Tg(mpeg1;dendra2)* transgenic zebrafish were used for macrophage analyses. (A,B) Immunofluorescence co-stain of PTs (red or green) and neutrophils (green) (A) and macrophages (red) (B) in gent-AKI+DMSO and gent-AKI +UPHD25. PTs are outlined in white and leukocytes are marked with arrows. (C) Quantification of neutrophil numbers showed no significance between DMSO and UPHD25 treatment groups. (D) Quantification of macrophage numbers showed a significant decrease in macrophage numbers in UPHD25 treatment group. Mean_{Gent-AKI+DMSO}=16.38 (N=69) vs Mean_{Gent-AKI+UPHD25}=12.99 (N=75). Data pooled from three biological replicates are shown expressed as mean±s.e.m. Two-tailed *t*-test: **P*<0.05, ns, not significant. Scale bars: 20 μm.

response with an increase in the number of dedifferentiated RTECs with a high proliferative potential.

Mouse studies have shown that PTBA treatment enhances recovery from AKI by influencing the innate immune response. After treating with the nephrotoxin aristolochic acid, Novitskaya et al. observed a late-AKI overall reduction in macrophage number that correlated with increased functional recovery and decreased fibrosis (Novitskaya et al., 2014). This is consistent with other reports of beneficial, anti-inflammatory properties of HDIs in kidney disease models (Venkatachalam et al., 2010; Wynn, 2010). In gent-AKI zebrafish, we saw a small but significant difference in the number of early infiltrating macrophages after treatment. These findings suggest that PTBA treatment may reduce the early innate immune response either by promoting a healthier microenvironment or by altering the response from an inflammatory (M1) to repair (M2) environment. In agreement with promoting a favorable repair environment, treatment was determined to both reduce Kim-1 expression in injured nephrons and decrease the number of M1 macrophages. No change in the number of M2 macrophages between treated and untreated larvae was observed, suggesting that PTBA likely does not play a direct role in promoting macrophage polarization from pro-inflammatory to pro-repair. However,

longitudinal studies may be needed to observe M2 conversion, as studies have shown that monocytes can infiltrate into sites of acute injury and differentiate into M2 macrophages at later time points (Dey et al., 2014). Overall, these findings indicate that PTBA improves the environment early during AKI events by promoting dedifferentiation/proliferation of tubular cells and preventing excessive pro-inflammatory peritubular macrophage recruitment.

We demonstrated that the pro-proliferative effects of PTBA on RTECs requires intact RA signaling. Activation of the RA pathway in RTECs has been shown to be a critical early step during the regenerative response, and HDACs are known to repress RA signaling (Brilli et al., 2013; Chiba et al., 2016). Thus, it is possible that PTBA may lower the threshold concentration of RA required to initiate the activation of downstream targets, or possibly prolong the window of active RA signaling (Menegola et al., 2006). Consistent with this idea, we showed that PTBA-enhanced proliferation only occurs in the context of injury and is dependent on intact RA signaling. The RA pathway is known to have a very early AKI response, within the first 24 hpi in zebrafish (Chiba et al., 2016). Since we are treating at 48 hpi, we know that the requirement for RA signaling is not an early, endogenous response, but is related to PTBA efficacy. This link between RA signaling and HDAC inhibition is best characterized in

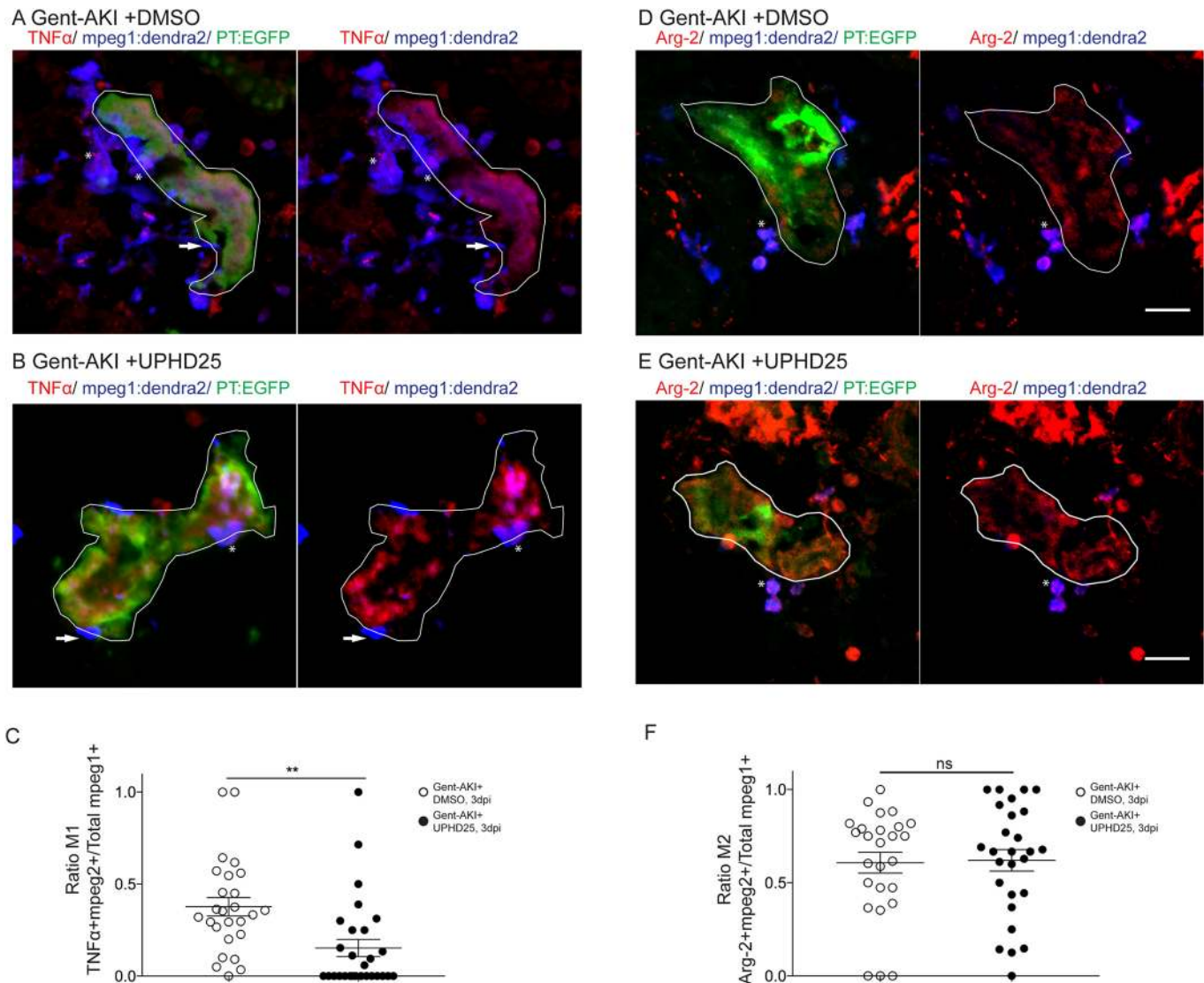


Fig. 6. UPHD25 treatment reduces total M1 macrophage population, but not M2 macrophage population. *Tg(mpeg1:dendra2); Tg(PT:EGFP)* transgenic zebrafish were used for macrophage polarization analysis. (A,B) Immunofluorescence co-stain of TNF α (red), macrophages (blue) and PT (green) in gent-AKI+DMSO (A) and gent-AKI+UPHD25 (B). PTs are outlined in white. TNF α +mpeg+ are marked with an asterisk and TNF α -mpeg1+ are marked with an arrow. (C) Quantification of M1 macrophage recruitment by counting TNF α +mpeg1+ cells adjacent to the PT. Mean $_{\text{Gent-AKI+DMSO}}=0.38$ ($N=26$) vs Mean $_{\text{Gent-AKI+UPHD25}}=0.15$ ($N=28$). (D,E) Immunofluorescence co-stain of arginase-2 (red), macrophages (blue) and PT (green) in gent-AKI+DMSO (D) and gent-AKI+UPHD25 (E). Arg2+/mpeg1+ are marked with an asterisk. (F) Quantification of M2 macrophage recruitment by counting Arg-2+/mpeg1+ cells adjacent to the PT. Mean $_{\text{Gent-AKI+DMSO}}=0.61$ ($N=26$) vs Mean $_{\text{Gent-AKI+UPHD25}}=0.62$ ($N=27$). Macrophage numbers were normalized by calculating the ratio of M1 or M2 over total macrophages; i.e. (TNF α +mpeg1+)/total mpeg1+. Data pooled from three biological replicates are shown expressed as mean \pm s.e.m. Two-tailed *t*-test: ** $P<0.01$, ns, not significant. Scale bars: 20 μ m.

cancer cells, where HDIs alter gene expression and restore sensitivity to retinoid treatment (Jiang et al., 2008; Rettig et al., 2015; Touma et al., 2005; Wang et al., 2005). In our current study, we demonstrate that RA and HDI treatment can also work together to improve kidney regeneration. However, it is not clear whether the RA signaling is directly downstream of PTBA activity, or whether there are other pathways involved. There are many important pathways that play a role in kidney regeneration, such as CREB, Wnt, TGF- β , Hippo and EGF (Arany et al., 2008, 2005; Chen et al., 2018; Kawakami et al., 2013; Tan et al., 2016; Xu et al., 2016). In future studies, it will be important to determine whether these pathways are actively engaged in driving PTBA efficacy.

Remote organ damage results in an increased risk of morbidity and mortality in AKI (Depret et al., 2017). The heart, liver, lung and brain

are frequently damaged during AKI via several pathways, such as inflammatory cascades, apoptosis and oxidative stress (Grams and Rabb, 2012; Nakazawa et al., 2017). Therefore, therapies that can target multiple organs will have greater therapeutic potential. Interestingly, we found that PTBA treatment can enhance cardiac regeneration by promoting cardiomyocyte proliferation and reducing fibrosis. Importantly, in uninjured hearts, PTBA does not increase cell proliferation, but has an effect only after cardiac injury. As with the kidney injury studies, we speculate that this is because RA production greatly increases in the zebrafish heart after injury to promote cardiomyocyte growth (Kikuchi et al., 2011). Future studies to determine the source of RA production will be necessary to understand whether there is a common cell type, such as immune cells, found in both the kidney and heart that mediates PTBA efficacy.

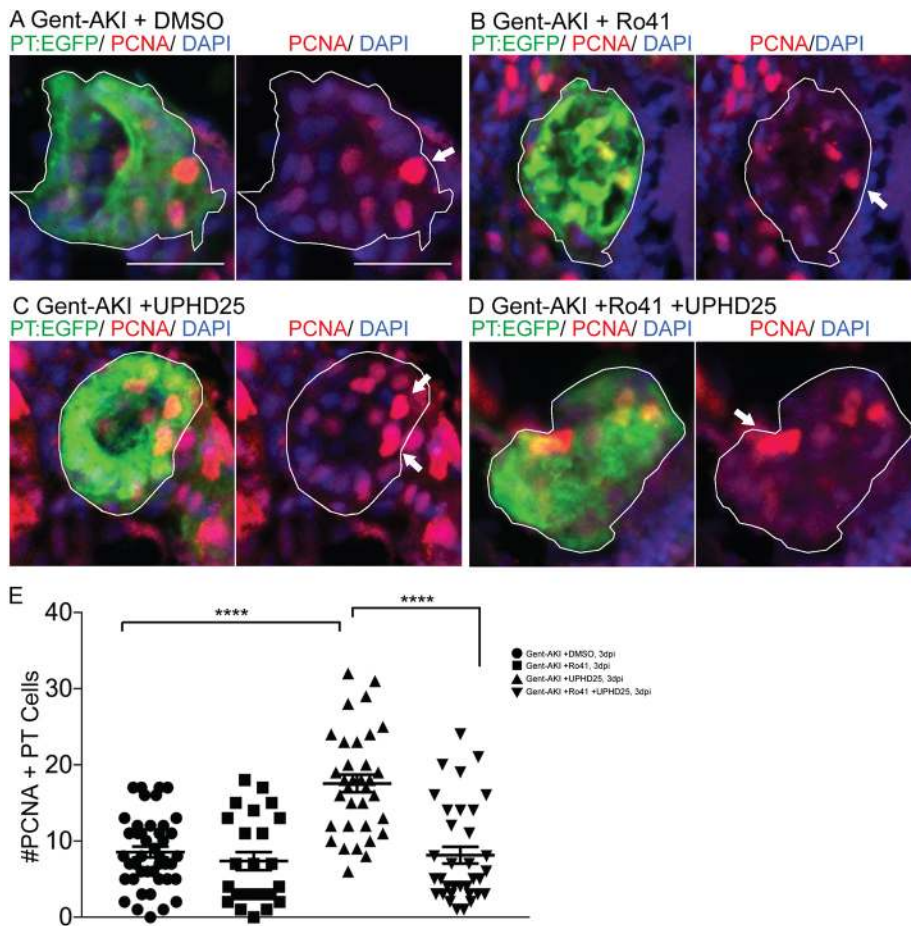


Fig. 7. UPHD25 treatment efficacy requires intact RA signaling. *Tg(PT:EGFP)* transgenic zebrafish were used to analyze RTEC proliferation. (A-D) Immunofluorescence stain showing cells actively undergoing S-phase marked with PCNA antibody (red) and PT (green) in gent-aki+DMSO (A), gent-aki+Ro41 (B), gent-aki+UPHD25 (C) and gent-aki+Ro41+UPHD25 (D). PTs are outlined in white and arrows mark PCNA+ RTECs. (E) Quantification of PCNA+ RTECs in each treatment group. Mean_{UPHD25}=17.56 (N=34) vs Mean_{Ro41+UPHD25}=8.15 (N=34). Data pooled from three biological replicates are shown expressed as mean±s.e.m. One-way ANOVA: *****P*<0.001. Scale bars: 20 μm.

Taken together, the current work provides a cellular mechanism for how PTBA accelerates renal recovery during AKI and cardiac regeneration. The goal of ongoing and future studies is to determine HDAC-isoform selectivity and ultimately the molecular targets of PTBA. The most likely target appears to be class I HDACs. One attractive candidate is HDAC8, which has been linked to the repression of the developmentally important renal transcription factor gene *Lhx1* (Haberland et al., 2009; Saha et al., 2013). Furthermore, HDAC8 has been connected to RA signaling in cancer. Combined treatment of neuroblastoma cells with all-trans RA and an HDAC8 inhibitor resulted in enhanced tumor cell death (Rettig et al., 2015). Ultimately, studies to characterize the HDAC-isoform selectivity and downstream molecular targets of PTBA will further our understanding of how this class of compound mitigates renal injury and advance efforts to develop a new drug therapy for AKI.

MATERIALS AND METHODS

Zebrafish husbandry

Studies were approved by the University of Pittsburgh IACUC. Zebrafish were maintained as described (Westerfield, 1993). In addition to AB wild-type, embryos were used from the following published transgenic lines: *Tg(PT:EGFP)^{nz4}* (Cianciolo Cosentino et al., 2013), *Tg(cdh17:mCherry)^{pt1307}* (Chiba et al., 2016), *Tg(lyz:EGFP)^{nz117}* (Kitaguchi et al., 2009) and *Tg(mpeg1:dendra2)^{uvml12}* (Harvie et al., 2013). For *in vivo* imaging, larvae were kept in E3 medium containing 0.003% 1-phenyl-2-thiourea (PTU) after 24 hpf. Both males and females were used for the study.

Generation of transgenic line *Tg(hsp70l:EGFP-HS-dnRARα)*

Tg(hsp70l:EGFP-HS-dnRARα) transgenic fish were generated by gateway-based Tol2 transposon transgenesis (Kwan et al., 2007). To generate the

transgenic fish, gateway cloning was used with the *hps70l* vector as the 5' entry clone and GFP-dnRARα, a previously reported human dominant negative RARα, as the middle entry clone (Pogoda et al., 2018; Waxman and Yelon, 2011). PolyA was used as the 3' entry clone. Constructs were injected into single-cell embryos and screened for insertion. In order to examine the effect of dnRAR during AKI, 2 dpi or 5 dpf zebrafish larvae were heat shocked at 37°C for 1 h. Then, the larvae were immediately treated with UPHD25 or DMSO.

Gentamicin-induced AKI

Zebrafish larvae were injected with a single dose of gentamicin as previously described (Cianciolo Cosentino et al., 2010). Briefly, larvae were anesthetized in 160 mg/ml tricaine (Sigma-Aldrich)/E3 medium and injected with a total of 1 nl gentamicin (8-12 ng) (Sigma-Aldrich) diluted in saline into the common cardinal vein. After injection, larvae were incubated in 50 μg/ml penicillin/streptomycin diluted in E3 medium.

Cardiac injury

Adult AB* or Tu wild-type zebrafish aged 6-18 months were anesthetized with tricaine then ventricle apex amputation was performed as previously described (Missinato et al., 2018).

Chemical treatments

All compounds were diluted in E3 medium containing 1% DMSO. UPHD25 was synthesized by Enamine and used at a working concentration of 1 μM. For RA inhibition studies, zebrafish larvae were treated with 1 μM Ro41-5253 (Enzo Life Sciences) in 1% DMSO diluted in E3 for 24 h from 3 to 4 dpf, and then compound was washed out with several changes of E3. In adults, either 3 μl of 50% DMSO vehicle in PBS or 200 μM UPHD25 was delivered by retro-orbital injection (Pugach et al., 2009). Injections were performed daily, from 1-6 dpa, and hearts were extracted at 7 dpa to assess cardiomyocyte proliferation, and at 20 dpa to measure scar size.

In situ hybridization

The *arginase-2* clone was synthesized and cloned into pEX-K248 with Sp6 promoter to drive the reverse transcription (Eurofins). *In situ* hybridizations were performed as previously described (de Groh et al., 2010). Larvae were cryosectioned and imaged using a 20× objective on an Axiovert 40 CFL brightfield scope (Zeiss). Images were captured using Axiovision Rel v4.8 software (Zeiss).

Histological analysis

Immunofluorescence microscopy was performed on cryosections as described previously (Drummond and Davidson, 2010). Larvae were fixed in 4% paraformaldehyde and treated with a 10–30% sucrose/PBS gradient before embedding in tissue freezing medium (Ted Pella). Sections were generated at a thickness of 12 μm. Slides were blocked with 10% goat serum in PBST (0.1% Tween-20), followed by primary and secondary antibody incubations. All antibodies used in this paper are annotated in Table S1. Incubation with DAPI (Vector Laboratories) was used to counterstain nuclei. The slides were washed with PBS then mounted with Aqua Polymount (Polysciences). Sections were examined by confocal microscopy (Zeiss LSM 700).

To quantify Pax2a-positive cells in *Tg(PT:EGFP)* fish, we imported serial images into ImageJ 1.46r software (NIH). The ROI tool was used to outline the kidney in the green channel, and ‘Analyze Particle’ function was used to quantify the number of Pax2a-positive cells in the red channel. Background and threshold values were constant between groups for each experiment. Particle size range was 80 to infinity. Per nephron, three images were analyzed. Similar ImageJ analysis was performed in *Tg(PT:EGFP); Tg(mpeg1:dendra2)* fish to quantify macrophage cell size. For these images, there was no background removal, *mpeg1:dendra2* channel threshold was 53–255, and particle size range was 60 to infinity.

Heart cryosections were stained with AFOG as previously described (Missinato et al., 2018). Images were captured with a Leica MZ 16 microscope and Q Imaging Retige 1300 camera. Clot area was measured using ImageJ (NIH).

Live confocal zebrafish imaging

At 24 h after gentamicin injection, *Tg(cdh17:mCherry); Tg(lyz:EGFP)* larvae were anesthetized in tricaine, embedded in a thin layer of 0.5% low-melt Sea Plaque agarose (Cambrex), and covered with E3 medium plus PTU to prevent pigment development. Image stacks were acquired using a Leica TCS SP5 multiphoton microscope (Leica Microsystems) with an HCX IRAPO L 20×/0.95 water immersion objective, non-descanned detectors and a custom-built motorized stage (Scientifica). Sequential stack scanning was performed bidirectionally with a resonant scanner (16,000 Hz, phase set to 1.69) with 32× line averaging and a zoom of 1.7×. EGFP and mCherry were excited with a Mai Tai DeepSee Ti:Sapphire laser (Newport/Spectra Physics) at 900 and 561 nm, respectively. Using the ‘Mark and Find’ function, (x,y) coordinates and z-series parameters (step size 1.48 μm) were defined for individual larvae. Images were captured every 27 min for 17 h. Maximal projections were compiled in series to generate time-lapse movies using LAS AF Version: 3.0.0 build 8134 and Metamorph software.

At 48 h after gentamicin injection, *Tg(cdh17:mCherry); Tg(mpeg1:dendra2)* larvae were processed for imaging using the protocol above. Image stacks were acquired using a Nikon Eclipse Ti confocal microscope (Nikon Instruments) with a 20× dry objective, and a motorized stage. Stacks were captured with 40 optical sections, with 5 μm step size. Dendra2 and mCherry were excited with 488 nm and 560 nm lasers, respectively. Dendra2 is photoconvertible with 488 nm and UV but maintains its original green fluorescence emission (509 nm) when imaged under laser power between 2 and 7%. Experiments utilizing *Tg(mpeg1:dendra2)* maintained low laser power to inhibit photoconversion from green to red. Using the ‘Mark and Find’ function, (x,y) coordinates and z-series parameters (5 μm) were defined for individual larvae. Images were captured every 90 min for 24 h. Maximal projections were compiled in series to generate time-lapse movies using Imaris image analysis software (Bitplane).

Zebrafish pronephros and RNA isolation

Tg(PT:EGFP) larvae at 6 dpf were used to collect GFP+ pronephros (N=100 for gent-AKI; N=100 for gent-AKI+UPHD25) as described (Drummond

and Davidson, 2010). All experiments were repeated three times. The larvae were incubated in 10 mM DTT in E3 and tricaine for 1.5–2 h at room temperature then with 5 mg/ml collagenase I in HBSS (Sigma-Aldrich) for 2.5–3.5 h at 32°C. The larvae were washed in Minimum Essential Media and 10% fetal calf serum (Gibco). Fine forceps and a p10 pipette were used to dissect GFP+ pronephros. The RNeasy Micro kit (Qiagen) was used for RNA isolation.

Library preparation and RNA sequencing

Total RNA (1 μg) underwent mRNA library preparation using TruSeq Stranded mRNA kit (Illumina), according to the manufacturer’s protocol. Final libraries were normalized to 10 nM, pooled and diluted. NextSeq 500 were seeded with 1.8 pM denatured library for automated cluster formation for approximately 30- to 40-million reads per sample.

RNA sequencing data analysis

We used Hisat2 (v2.1.0) (Kim et al., 2015) to align paired-end RNA-seq reads to the zebrafish reference genome (UCSC danRer11) and gene-level counts per million (CPM) were calculated using featureCounts (Liao et al., 2014) and edgeR (Robinson et al., 2010).

Statistical analysis

Data were analyzed using Student’s *t*-test, one-way ANOVA, and two-way ANOVA as indicated, and data are reported as mean±s.e.m. *P*-values were considered significant when <0.05. For studies in zebrafish larvae, *N* reflects the number of nephrons included in the analysis per group. When visible, both nephrons per fish were included. For adult zebrafish studies, *N* reflects the number of hearts included per group.

Acknowledgements

We thank the Huttenlocher lab for the *Tg(mpeg1:dendra2)* line, and the University of Pittsburgh HSCRF Health Sciences Sequencing Core at Children’s Hospital for RNA library preparation and RNA-sequencing.

Competing interests

The authors declare no competing or financial interests.

Author contributions

Conceptualization: L.B.S., H.I.H., E.B.E., M.A.M., S.C.W., A.J.D., M.T., N.A.H.; Methodology: L.B.S., H.I.H., E.B.E., M.A.M., E.R.R., M.D.M., A.S.B., B.L.R., J.S.W., S.C.W., A.J.D., M.T., N.A.H.; Validation: M.D.M., M.T., N.A.H.; Formal analysis: L.B.S., H.I.H., E.B.E., M.A.M., M.D.M., A.S.B., M.T., N.A.H.; Investigation: L.B.S., H.I.H., E.B.E., M.A.M., E.R.R., M.D.M.; Data curation: A.S.B.; Writing - original draft: L.B.S., H.I.H., E.B.E., A.S.B.; Writing - review & editing: L.B.S., H.I.H., E.B.E., M.A.M., E.R.R., B.L.R., J.S.W., S.C.W., A.J.D., M.T.; Visualization: L.B.S., H.I.H., E.B.E., N.A.H.; Supervision: B.L.R., M.T., N.A.H.; Project administration: N.A.H.; Funding acquisition: A.J.D., M.T., N.A.H.

Funding

This research was funded by the National Institutes of Health [2R01DK069403, 1R01DK112652, 1P30DK079307 to N.A.H., F30DK101143 to L.B.S., T32DK061296 to E.B.E., R01HD053287 to M.T.]; the U.S. Department of Defense [W81XWH-17-1-0610 to N.A.H.]; the Health Research Council of New Zealand [15/057 & 17/425 to A.J.D.]; and the American Heart Association [14GRNT20480183 to M.T.].

Data availability

The RNA-seq data has been deposited in the Gene Expression Omnibus repository with the accession number GSE126418.

Supplementary information

Supplementary information available online at <http://dmm.biologists.org/lookup/doi/10.1242/dmm.037390.supplemental>

References

- Arany, I., Megyesi, J. K., Reusch, J. E. B. and Safirstein, R. L. (2005). CREB mediates ERK-induced survival of mouse renal tubular cells after oxidant stress. *Kidney Int.* **68**, 1573–1582.
- Arany, I., Herbert, J., Herbert, Z. and Safirstein, R. L. (2008). Restoration of CREB function ameliorates cisplatin cytotoxicity in renal tubular cells. *Am. J. Physiol. Renal. Physiol.* **294**, F577–F581.

- Awad, A. S., Rouse, M., Huang, L., Vergis, A. L., Reutershan, J., Cathro, H. P., Linden, J. and Okusa, M. D. (2009). Compartmentalization of neutrophils in the kidney and lung following acute ischemic kidney injury. *Kidney Int.* **75**, 689-698.
- Bagshaw, S. M., George, C., Bellomo, R. and Committe, A. D. M. (2008). A comparison of the RIFLE and AKIN criteria for acute kidney injury in critically ill patients. *Nephrol. Dial. Transplant.* **23**, 1569-1574.
- Benigni, A., Morigi, M. and Remuzzi, G. (2010). Kidney regeneration. *Lancet* **375**, 1310-1317.
- Bonventre, J. V. (2003). Dedifferentiation and proliferation of surviving epithelial cells in acute renal failure. *J. Am. Soc. Nephrol.* **14** Suppl. 1, S55-S61.
- Brilli, L. L., Swanhart, L. M., de Caestecker, M. P. and Hukriede, N. A. (2013). HDAC inhibitors in kidney development and disease. *Pediatr. Nephrol.* **28**, 1909-1921.
- Cao, Q., Harris, D. C. H. and Wang, Y. (2015). Macrophages in kidney injury, inflammation, and fibrosis. *Physiology* **30**, 183-194.
- Chawla, L. S. and Kimmel, P. L. (2012). Acute kidney injury and chronic kidney disease: an integrated clinical syndrome. *Kidney Int.* **82**, 516-524.
- Chen, J., You, H., Li, Y., Xu, Y., He, Q. and Harris, R. C. (2018). EGF receptor-dependent YAP activation is important for renal recovery from AKI. *J. Am. Soc. Nephrol.* **29**, 2372-2385.
- Chertow, G. M., Burdick, E., Honour, M., Bonventre, J. V. and Bates, D. W. (2005). Acute kidney injury, mortality, length of stay, and costs in hospitalized patients. *J. Am. Soc. Nephrol.* **16**, 3365-3370.
- Chiba, T., Skrypnik, N. I., Skvarca, L. B., Penchev, R., Zhang, K. X., Rochon, E. R., Fall, J. L., Paueksakorn, P., Yang, H., Alford, C. E. et al. (2016). Retinoic acid signaling coordinates macrophage-dependent injury and repair after AKI. *J. Am. Soc. Nephrol.* **27**, 495-508.
- Cianciolo Cosentino, C., Roman, B. L., Drummond, I. A. and Hukriede, N. A. (2010). Intravenous microinjections of zebrafish larvae to study acute kidney injury. *J. Vis. Exp.*, e2079.
- Cianciolo Cosentino, C., Skrypnik, N. I., Brilli, L. L., Chiba, T., Novitskaya, T., Woods, C., West, J., Korotchenko, V. N., McDermott, L., Day, B. W. et al. (2013). Histone deacetylase inhibitor enhances recovery after AKI. *J. Am. Soc. Nephrol.* **24**, 943-953.
- Cirio, M. C., de Groh, E. D., de Caestecker, M. P., Davidson, A. J. and Hukriede, N. A. (2014). Kidney regeneration: common themes from the embryo to the adult. *Pediatr. Nephrol.* **29**, 553-564.
- Coca, S. G., Singanamala, S. and Parikh, C. R. (2012). Chronic kidney disease after acute kidney injury: a systematic review and meta-analysis. *Kidney Int.* **81**, 442-448.
- Cruz, D. N., Bolgan, I., Perazella, M. A., Bonello, M., de Cal, M., Corradi, V., Polanco, N., Ocampo, C., Nalesso, F., Piccinni, P. et al. (2007). North East Italian Prospective Hospital Renal Outcome Survey on Acute Kidney Injury (NEIPHROS-AKI): targeting the problem with the RIFLE Criteria. *Clin. J. Am. Soc. Nephrol.* **2**, 418-425.
- de Groh, E. D., Swanhart, L. M., Cosentino, C. C., Jackson, R. L., Dai, W., Kitchens, C. A., Day, B. W., Smithgall, T. E. and Hukriede, N. A. (2010). Inhibition of histone deacetylase expands the renal progenitor cell population. *J. Am. Soc. Nephrol.* **21**, 794-802.
- Depret, F., Prud'homme, M. and Legrand, M. (2017). A role of remote organs effect in acute kidney injury outcome? *Nephron* **137**, 273-276.
- Dey, A., Allen, J. and Hankey-Giblin, P. A. (2014). Ontogeny and polarization of macrophages in inflammation: blood monocytes versus tissue macrophages. *Front. Immunol.* **5**, 683.
- Drummond, I. A. and Davidson, A. J. (2010). Zebrafish kidney development. *Methods Cell Biol.* **100**, 233-260.
- Ellett, F., Pase, L., Hayman, J. W., Andrianopoulos, A. and Lieschke, G. J. (2011). mpeg1 promoter transgenes direct macrophage-lineage expression in zebrafish. *Blood* **117**, e49-e56.
- Fang, Y., Ding, X., Zhong, Y., Zou, J., Teng, J., Tang, Y., Lin, J. and Lin, P. (2010). Acute kidney injury in a Chinese hospitalized population. *Blood Purif.* **30**, 120-126.
- Fass, D. M., Shah, R., Ghosh, B., Hennig, K., Norton, S., Zhao, W.-N., Reis, S. A., Klein, P. S., Mazitschek, R., Maglathlin, R. L. et al. (2011). Short-chain HDAC inhibitors differentially affect vertebrate development and neuronal chromatin. *ACS Med. Chem. Lett.* **2**, 39-42.
- Ferenbach, D. A. and Bonventre, J. V. (2015). Mechanisms of maladaptive repair after AKI leading to accelerated kidney ageing and CKD. *Nat. Rev. Nephrol.* **11**, 264-276.
- Grams, M. E. and Rabb, H. (2012). The distant organ effects of acute kidney injury. *Kidney Int.* **81**, 942-948.
- Grande, M. T., Sánchez-Laorden, B., López-Blau, C., De Frutos, C. A., Boutet, A., Arévalo, M., Rowe, R. G., Weiss, S. J., López-Novoa, J. M. and Nieto, M. A. (2015). Snail1-induced partial epithelial-to-mesenchymal transition drives renal fibrosis in mice and can be targeted to reverse established disease. *Nat. Med.* **21**, 989-997.
- Haberland, M., Mokalled, M. H., Montgomery, R. L. and Olson, E. N. (2009). Epigenetic control of skull morphogenesis by histone deacetylase 8. *Genes Dev.* **23**, 1625-1630.
- Han, H. I., Skvarca, L. B., Espiritu, E. B., Davidson, A. J. and Hukriede, N. A. (2019). The role of macrophages during acute kidney injury: destruction and repair. *Pediatr. Nephrol.* **34**, 561-569.
- Harvie, E. A., Green, J. M., Neely, M. N. and Huttenlocher, A. (2013). Innate immune response to *Streptococcus iniae* infection in zebrafish larvae. *Infect. Immun.* **81**, 110-121.
- He, S., Liu, N., Bayliss, G. and Zhuang, S. (2013). EGFR activity is required for renal tubular cell dedifferentiation and proliferation in a murine model of folic acid-induced acute kidney injury. *Am. J. Physiol. Renal. Physiol.* **304**, F356-F366.
- Hentschel, D. M., Park, K. M., Cilenti, L., Zervos, A. S., Drummond, I. and Bonventre, J. V. (2005). Acute renal failure in zebrafish: a novel system to study a complex disease. *Am. J. Physiol. Renal. Physiol.* **288**, F923-F929.
- Hoste, E. A. J., Clermont, G., Kersten, A., Venkataraman, R., Angus, D. C., De Bacquer, D. and Kellum, J. A. (2006). RIFLE criteria for acute kidney injury are associated with hospital mortality in critically ill patients: a cohort analysis. *Crit. Care* **10**, R73.
- Humphreys, B. D., Valerius, M. T., Kobayashi, A., Mugford, J. W., Soeung, S., Duffield, J. S., McMahon, A. P. and Bonventre, J. V. (2008). Intrinsic epithelial cells repair the kidney after injury. *Cell Stem Cell* **2**, 284-291.
- Humphreys, B. D., Czerniak, S., DiRocco, D. P., Hasnain, W., Cheema, R. and Bonventre, J. V. (2011). Repair of injured proximal tubule does not involve specialized progenitors. *Proc. Natl. Acad. Sci. USA* **108**, 9226-9231.
- Humphreys, B. D., Xu, F., Sabbisetti, V., Rrgic, I., Naini, S. M., Wang, N., Chen, G., Xiao, S., Patel, D., Henderson, J. M. et al. (2013). Chronic epithelial kidney injury molecule-1 expression causes murine kidney fibrosis. *J. Clin. Invest.* **123**, 4023-4035.
- Ichimura, T., Bonventre, J. V., Bailly, V., Wei, H., Hession, C. A., Cate, R. L. and Sanicola, M. (1998). Kidney injury molecule-1 (KIM-1), a putative epithelial cell adhesion molecule containing a novel immunoglobulin domain, is up-regulated in renal cells after injury. *J. Biol. Chem.* **273**, 4135-4142.
- Imgrund, M., Gröne, E., Gröne, H.-J., Kretzler, M., Holzman, L., Schlöndorff, D. and Rothenpieler, U. W. (1999). Re-expression of the developmental gene Pax-2 during experimental acute tubular necrosis in mice 1. *Kidney Int.* **56**, 1423-1431.
- Jiang, M., Zhu, K., Grenet, J. and Lahti, J. M. (2008). Retinoic acid induces caspase-8 transcription via phospho-CREB and increases apoptotic responses to death stimuli in neuroblastoma cells. *Biochim. Biophys. Acta* **1783**, 1055-1067.
- Jo, S.-K., Sung, S.-A., Cho, W.-Y., Go, K.-J. and Kim, H.-K. (2006). Macrophages contribute to the initiation of ischaemic acute renal failure in rats. *Nephrol. Dial. Transplant.* **21**, 1231-1239.
- Jopling, C., Sleep, E., Raya, M., Martí, M., Raya, A. and Izpisua Belmonte, J. C. (2010). Zebrafish heart regeneration occurs by cardiomyocyte dedifferentiation and proliferation. *Nature* **464**, 606-609.
- Kawakami, T., Ren, S. and Duffield, J. S. (2013). Wnt signalling in kidney diseases: dual roles in renal injury and repair. *J. Pathol.* **229**, 221-231.
- Keightley, M.-C., Wang, C.-H., Pazhakh, V. and Lieschke, G. J. (2014). Delineating the roles of neutrophils and macrophages in zebrafish regeneration models. *Int. J. Biochem. Cell Biol.* **56**, 92-106.
- Kellum, J. A. and Chawla, L. S. (2016). Cell-cycle arrest and acute kidney injury: the light and the dark sides. *Nephrol. Dial. Transplant.* **31**, 16-22.
- Kelly, K. J., Williams, W. W., Jr., Colvin, R. B., Meehan, S., Springer, T. A., Gutierrez-Ramos, J. C. and Bonventre, J. V. (1996). Intercellular adhesion molecule-1-deficient mice are protected against ischemic renal injury. *J. Clin. Invest.* **97**, 1056-1063.
- Kikuchi, K., Holdway, J. E., Werdich, A. A., Anderson, R. M., Fang, Y., Egnaczyk, G. F., Evans, T., Macrae, C. A., Stainier, D. Y. R. and Poss, K. D. (2010). Primary contribution to zebrafish heart regeneration by gata4(+) cardiomyocytes. *Nature* **464**, 601-605.
- Kikuchi, K., Holdway, J. E., Major, R. J., Blum, N., Dahn, R. D., Begemann, G. and Poss, K. D. (2011). Retinoic acid production by endocardium and epicardium is an injury response essential for zebrafish heart regeneration. *Dev. Cell* **20**, 397-404.
- Kim, D., Langmead, B. and Salzberg, S. L. (2015). HISAT: a fast spliced aligner with low memory requirements. *Nat. Methods* **12**, 357-360.
- Kinugasa, F., Noto, T., Matsuoka, H., Urano, Y., Sudo, Y., Takakura, S. and Mutoh, S. (2010). Prevention of renal interstitial fibrosis via histone deacetylase inhibition in rats with unilateral ureteral obstruction. *Transpl. Immunol.* **23**, 18-23.
- Kitaguchi, T., Kawakami, K. and Kawahara, A. (2009). Transcriptional regulation of a myeloid-lineage specific gene lysozyme C during zebrafish myelopoiesis. *Mech. Dev.* **126**, 314-323.
- Kjellstrand, C. M., Ebben, J. and Davin, T. (1981). Time of death, recovery of renal function, development of chronic renal failure and need for chronic hemodialysis in patients with acute tubular necrosis. *Trans. Am. Soc. Artif. Intern. Organs* **27**, 45-50.
- Kwan, K. M., Fujimoto, E., Grabher, C., Mangum, B. D., Hardy, M. E., Campbell, D. S., Parant, J. M., Yost, H. J., Kanki, J. P. and Chien, C.-B. (2007). The Tol2kit: a multisite gateway-based construction kit for Tol2 transposon transgenesis constructs. *Dev. Dyn.* **236**, 3088-3099.
- Lee, S., Huen, S., Nishio, H., Nishio, S., Lee, H. K., Choi, B.-S., Ruhrberg, C. and Cantley, L. G. (2011). Distinct macrophage phenotypes contribute to kidney injury and repair. *J. Am. Soc. Nephrol.* **22**, 317-326.

- Levey, A. S. and James, M. T. (2017). Acute Kidney Injury. *Ann. Intern. Med.* **167**, ITC66-ITC80.
- Li, L., Huang, L., Sung, S.-S. J., Vergis, A. L., Rosin, D. L., Rose, C. E., Jr., Lobo, P. I. and Okusa, M. D. (2008). The chemokine receptors CCR2 and CX3CR1 mediate monocyte/macrophage trafficking in kidney ischemia-reperfusion injury. *Kidney Int.* **74**, 1526-1537.
- Liaño, F., Felipe, C., Tenorio, M.-T., Rivera, M., Abraira, V., Sáez-de-Urturi, J.-M., Ocaña, J., Fuentes, C. and Severiano, S. (2007). Long-term outcome of acute tubular necrosis: a contribution to its natural history. *Kidney Int.* **71**, 679-686.
- Liao, Y., Smyth, G. K. and Shi, W. (2014). featureCounts: an efficient general purpose program for assigning sequence reads to genomic features. *Bioinformatics* **30**, 923-930.
- Lieberthal, W. and Nigam, S. K. (2000). Acute renal failure. II. Experimental models of acute renal failure: imperfect but indispensable. *Am. J. Physiol. Renal. Physiol.* **278**, F1-F12.
- Lin, S.-L., Li, B., Rao, S., Yeo, E.-J., Hudson, T. E., Nowlin, B. T., Pei, H., Chen, L., Zheng, J. J., Carroll, T. J. et al. (2010). Macrophage Wnt7b is critical for kidney repair and regeneration. *Proc. Natl. Acad. Sci. USA* **107**, 4194-4199.
- Liu, N., He, S., Ma, L., Ponnusamy, M., Tang, J., Tolbert, E., Bayliss, G., Zhao, T. C., Yan, H. and Zhuang, S. (2013). Blocking the class I histone deacetylase ameliorates renal fibrosis and inhibits renal fibroblast activation via modulating TGF-beta and EGFR signaling. *PLoS ONE* **8**, e54001.
- Lovisa, S., LeBleu, V. S., Tampe, B., Sugimoto, H., Vagnagara, K., Carstens, J. L., Wu, C.-C., Hagos, Y., Burckhardt, B. C., Pentcheva-Hoang, T. et al. (2015). Epithelial-to-mesenchymal transition induces cell cycle arrest and parenchymal damage in renal fibrosis. *Nat. Med.* **21**, 998-1009.
- Maeshima, A., Maeshima, K., Nojima, Y. and Kojima, I. (2002). Involvement of Pax-2 in the action of activin A on tubular cell regeneration. *J. Am. Soc. Nephrol.* **13**, 2850-2859.
- Marumo, T., Hishikawa, K., Yoshikawa, M., Hirahashi, J., Kawachi, S. and Fujita, T. (2010). Histone deacetylase modulates the proinflammatory and -fibrotic changes in tubulointerstitial injury. *Am. J. Physiol. Renal. Physiol.* **298**, F133-F141.
- Menegola, E., Di Renzo, F., Broccia, M. L. and Giavini, E. (2006). Inhibition of histone deacetylase as a new mechanism of teratogenesis. *Birth Defects Res. C Embryo Today* **78**, 345-353.
- Missinato, M. A., Tobita, K., Romano, N., Carroll, J. A. and Tsang, M. (2015). Extracellular component hyaluronic acid and its receptor Hmhr are required for epicardial EMT during heart regeneration. *Cardiovasc. Res.* **107**, 487-498.
- Missinato, M. A., Saydmohammed, M., Zuppo, D. A., Rao, K. S., Opie, G. W., Kühn, B. and Tsang, M. (2018). Dusp6 attenuates Ras/MAPK signaling to limit zebrafish heart regeneration. *Development* **145**, dev157206.
- Murugan, R. and Kellum, J. A. (2011). Acute kidney injury: what's the prognosis? *Nat. Rev. Nephrol.* **7**, 209-217.
- Nakazawa, D., Kumar, S. V., Marschner, J., Desai, J., Holderried, A., Rath, L., Kraft, F., Lei, Y., Fukasawa, Y., Moeckel, G. W. et al. (2017). Histones and Neutrophil Extracellular Traps Enhance Tubular Necrosis and Remote Organ Injury in Ischemic AKI. *J. Am. Soc. Nephrol.* **28**, 1753-1768.
- Nelson, A., Schneider, D. M., Takatoh, J., Sakurai, K., Wang, F. and Mooney, R. (2013). A circuit for motor cortical modulation of auditory cortical activity. *J. Neurosci.* **33**, 14342-14353.
- Nguyen-Chi, M., Laplace-Builhe, B., Travnickova, J., Luz-Crawford, P., Tejedor, G., Phan, Q. T., Duroux-Richard, I., Levraud, J.-P., Kissa, K., Lutfalla, G. et al. (2015). Identification of polarized macrophage subsets in zebrafish. *eLife* **4**, e07288.
- Novitskaya, T., McDermott, L., Zhang, K. X., Chiba, T., Paueksakon, P., Hukriede, N. A. and de Caestecker, M. P. (2014). A PTBA small molecule enhances recovery and reduces postinjury fibrosis after aristolochic acid-induced kidney injury. *Am. J. Physiol. Renal. Physiol.* **306**, F496-F504.
- Ostermann, M. and Chang, R. (2007). Acute kidney injury in the intensive care unit according to RIFLE. *Crit. Care Med.* **35**, 1837-1843; quiz 1852.
- Pogoda, H.-M., Riedl-Quinkertz, I., Löhr, H., Waxman, J. S., Dale, R. M., Topczewski, J., Schulte-Merker, S. and Hammerschmidt, M. (2018). Direct activation of chondroblasts by retinoic acid is required for segmented centra mineralization during zebrafish spine development. *Development* **145**, dev159418.
- Poss, K. D., Wilson, L. G. and Keating, M. T. (2002). Heart regeneration in zebrafish. *Science* **298**, 2188-2190.
- Pugach, E. K., Li, P., White, R. and Zon, L. (2009). Retro-orbital injection in adult zebrafish. *J. Vis. Exp.*, e1645.
- Rabb, H., Mendiola, C. C., Dietz, J., Saba, S. R., Issekutz, T. B., Abanilla, F., Bonventre, J. V. and Ramirez, G. (1994). Role of CD11a and CD11b in ischemic acute renal failure in rats. *Am. J. Physiol.* **267**, F1052-F1058.
- Rettig, I., Koeneke, E., Trippel, F., Mueller, W. C., Burhenne, J., Kopp-Schneider, A., Fabian, J., Schober, A., Fernekorn, U., von Deimling, A. et al. (2015). Selective inhibition of HDAC8 decreases neuroblastoma growth in vitro and in vivo and enhances retinoic acid-mediated differentiation. *Cell Death Dis.* **6**, e1657.
- Ricardo, S. D., van Goor, H. and Eddy, A. A. (2008). Macrophage diversity in renal injury and repair. *J. Clin. Invest.* **118**, 3522-3530.
- Robinson, M. D., McCarthy, D. J. and Smyth, G. K. (2010). edgeR: a Bioconductor package for differential expression analysis of digital gene expression data. *Bioinformatics* **26**, 139-140.
- Saha, A., Pandian, G. N., Sato, S., Taniguchi, J., Hashiya, K., Bando, T. and Sugiyama, H. (2013). Synthesis and biological evaluation of a targeted DNA-binding transcriptional activator with HDAC8 inhibitory activity. *Bioorg. Med. Chem.* **21**, 4201-4209.
- Sanker, S., Cirio, M. C., Vollmer, L. L., Goldberg, N. D., McDermott, L. A., Hukriede, N. A. and Vogt, A. (2013). Development of high-content assays for kidney progenitor cell expansion in transgenic zebrafish. *J. Biomol. Screen.* **18**, 1193-1202.
- Schmidt, I. M., Hall, I. E., Kale, S., Lee, S., He, C.-H., Lee, Y., Chupp, G. L., Moeckel, G. W., Lee, C. G., Elias, J. A. et al. (2013). Chitinase-like protein Brp-39/YKL-40 modulates the renal response to ischemic injury and predicts delayed allograft function. *J. Am. Soc. Nephrol.* **24**, 309-319.
- Skrypnik, N. I., Sanker, S., Skvarca, L. B., Novitskaya, T., Woods, C., Chiba, T., Patel, K., Goldberg, N. D., McDermott, L., Vinson, P. N. et al. (2016). Delayed treatment with PTBA analogs reduces postinjury renal fibrosis after kidney injury. *Am. J. Physiol. Renal. Physiol.* **310**, F705-F716.
- Sola, A., Weigert, A., Jung, M., Vinuesa, E., Brecht, K., Weis, N., Brüne, B., Borregaard, N. and Hotter, G. (2011). Sphingosine-1-phosphate signalling induces the production of Lcn-2 by macrophages to promote kidney regeneration. *J. Pathol.* **225**, 597-608.
- Tan, R. J., Zhou, D. and Liu, Y. (2016). Signaling crosstalk between tubular epithelial cells and interstitial fibroblasts after kidney injury. *Kidney Dis.* **2**, 136-144.
- Terada, Y., Tanaka, H., Okado, T., Shimamura, H., Inoshita, S., Kuwahara, M. and Sasaki, S. (2003). Expression and function of the developmental gene Wnt-4 during experimental acute renal failure in rats. *J. Am. Soc. Nephrol.* **14**, 1223-1233.
- Thornton, M. A., Winn, R., Alpers, C. E. and Zager, R. A. (1989). An evaluation of the neutrophil as a mediator of in vivo renal ischemic-reperfusion injury. *Am. J. Pathol.* **135**, 509-515.
- Touma, S. E., Goldberg, J. S., Moench, P., Guo, X., Tickoo, S. K., Gudas, L. J. and Nanus, D. M. (2005). Retinoic acid and the histone deacetylase inhibitor trichostatin A inhibit the proliferation of human renal cell carcinoma in a xenograft tumor model. *Clin. Cancer Res.* **11**, 3558-3566.
- Uchino, S., Bellomo, R., Goldsmith, D., Bates, S. and Ronco, C. (2006). An assessment of the RIFLE criteria for acute renal failure in hospitalized patients. *Crit. Care Med.* **34**, 1913-1917.
- Varmeh, S., Egia, A., McGrouther, D., Tahan, S. R., Bayat, A. and Pandolfi, P. P. (2011). Cellular senescence as a possible mechanism for halting progression of keloid lesions. *Genes Cancer* **2**, 1061-1066.
- Venkatachalam, M. A., Griffin, K. A., Lan, R., Geng, H., Saikumar, P. and Bidani, A. K. (2010). Acute kidney injury: a springboard for progression in chronic kidney disease. *Am. J. Physiol. Renal. Physiol.* **298**, F1078-F1094.
- Villanueva, S., Céspedes, C. and Vio, C. P. (2006). Ischemic acute renal failure induces the expression of a wide range of nephrogenic proteins. *Am. J. Physiol. Regul. Integr. Comp. Physiol.* **290**, R861-R870.
- Wang, X.-F., Qian, D. Z., Ren, M., Kato, Y., Wei, Y., Zhang, L., Fansler, Z., Clark, D., Nakanishi, O. and Pili, R. (2005). Epigenetic modulation of retinoic acid receptor beta2 by the histone deacetylase inhibitor MS-275 in human renal cell carcinoma. *Clin. Cancer Res.* **11**, 3535-3542.
- Wang, W. E., Li, L., Xia, X., Fu, W., Liao, Q., Lan, C., Yang, D., Chen, H., Yue, R., Zeng, C. et al. (2017). Dedifferentiation, proliferation, and redifferentiation of adult mammalian cardiomyocytes after Ischemic injury. *Circulation* **136**, 834-848.
- Waxman, J. S. and Yelon, D. (2011). Zebrafish retinoic acid receptors function as context-dependent transcriptional activators. *Dev. Biol.* **352**, 128-140.
- Waxman, J. S., Keegan, B. R., Roberts, R. W., Poss, K. D. and Yelon, D. (2008). Hoxb5b acts downstream of retinoic acid signaling in the forelimb field to restrict heart field potential in zebrafish. *Dev. Cell* **15**, 923-934.
- Westerfield, M. (1993). *The Zebrafish Book: A Guide for the Laboratory Use of Zebrafish (Brachydanio rerio)*. Eugene, OR: M. Westerfield.
- Wiegertjes, G. F., Wentzel, A. S., Spaik, H. P., Elks, P. M. and Fink, I. R. (2016). Polarization of immune responses in fish: the 'macrophages first' point of view. *Mol. Immunol.* **69**, 146-156.
- Witzgall, R., Brown, D., Schwarz, C. and Bonventre, J. V. (1994). Localization of proliferating cell nuclear antigen, vimentin, c-Fos, and clusterin in the postischemic kidney. Evidence for a heterogeneous genetic response among nephron segments, and a large pool of mitotically active and dedifferentiated cells. *J. Clin. Invest.* **93**, 2175-2188.
- Wolfs, T. G., Buurman, W. A., van Schadewijk, A., de Vries, B., Daemen, M. A., Hiemstra, P. S. and van 't Veer, C. (2002). In vivo expression of Toll-like receptor 2 and 4 by renal epithelial cells: IFN-gamma and TNF-alpha mediated up-regulation during inflammation. *J. Immunol.* **168**, 1286-1293.
- Wu, H., Chen, G., Wyburn, K. R., Yin, J., Bertolino, P., Eris, J. M., Alexander, S. I., Sharland, A. F. and Chadban, S. J. (2007). TLR4 activation mediates kidney ischemia/reperfusion injury. *J. Clin. Invest.* **117**, 2847-2859.
- Wynn, T. A. (2010). Fibrosis under arrest. *Nat. Med.* **16**, 523-525.

- Xu, J., Li, P.-X., Wu, J., Gao, Y.-J., Yin, M.-X., Lin, Y., Yang, M., Chen, D.-P., Sun, H.-P., Liu, Z.-B. et al.** (2016). Involvement of the Hippo pathway in regeneration and fibrogenesis after ischaemic acute kidney injury: YAP is the key effector. *Clin. Sci. (Lond.)* **130**, 349-363.
- Yang, L., Besschetnova, T. Y., Brooks, C. R., Shah, J. V. and Bonventre, J. V.** (2010). Epithelial cell cycle arrest in G2/M mediates kidney fibrosis after injury. *Nat. Med.* **16**, 535-543, 1p following 143.
- Zahedi, K., Revelo, M. P., Barone, S., Wang, Z., Tehrani, K., Citron, D. P., Bissler, J. J., Rabb, H. and Soleimani, M.** (2006). Stathmin-deficient mice develop fibrosis and show delayed recovery from ischemic-reperfusion injury. *Am. J. Physiol. Renal. Physiol.* **290**, F1559-F1567.
- Zhang, M.-Z., Yao, B., Yang, S., Jiang, L., Wang, S., Fan, X., Yin, H., Wong, K., Miyazawa, T., Chen, J. et al.** (2012). CSF-1 signaling mediates recovery from acute kidney injury. *J. Clin. Invest.* **122**, 4519-4532.